Supporting information

Thermally activated delayed fluorescence from Ag(I) complexes: A route to 100% quantum yield at unprecedentedly short decay time

Marsel Z. Shafikov[†,‡], Alfiya F. Suleymanova[†,¥], Rafał Czerwieniec[†], and Hartmut Yersin[†]*

[†] Institut für Physikalische und Theoretische Chemie, Universität Regensburg, Universitätsstrasse 31, D-93053 Regensburg, Germany
[‡] Ural Federal University, Mira 19, Ekaterinburg, 620002, Russia
[¥] I. Postovsky Institute of Organic Synthesis, Ekaterinburg, 620041, Russia

Contents **Pages**

Experimental.
NMR spectra were recorded on a Bruker AVANCE spectrometer operating at 300 MHz for ^{1}H and 121.5 MHz for ^{31}P with residual protic solvent used as internal standard.

Syntheses.
***Bis*-(diphenylphosphine)-*ortho*-carborane.** Synthesis was carried out in two steps starting from commercially available *ortho*-carborane, *n*-butyl-lithium (n-BuLi), and diphenylphosphine chloride. A 1.6 M solution of n-BuLi in hexane (2.9 ml, 4.68 mmol) was added to a solution of *ortho*-carborane (0.3 g, 2.08 mmol) in diethyl ether at 0 °C and stirred at room temperature for 30 min and then refluxed for 30 min. The solution was cooled to 0 °C and diphenylphosphine chloride (0.95 ml, 5.2 mmol) was added dropwise. The mixture was stirred at room temperature for 30 min and quenched with a saturated aqueous solution of ammonium chloride. The mixture was extracted with diethyl ether, organic phases were combined, washed with brine, and dried over $MgSO_4$. The solvent removed in vacuo and the residue purified by column chromatography (silica gel, CH_2Cl_2) that afforded the product as colorless solid. Yield 55 %. ^{1}H NMR ($CDCl_3$): 7.9-7.79 (m, 8H), 7.50-7.36 (m, 12H), 3.0-1.5 (br, 10H). ^{31}P NMR ($CDCl_3$): 7.82 ppm.

Ag(phen)(P_2-nCB). To a solution of $AgPF_6$ (49 mg, 0.195 mmol) in ethanol *bis*-(diphenylphosphine)-*ortho*-carborane (100 mg, 0.195 mmol) was added and the mixture was stirred at room temperature for 1 hour. Then 1,10-phenanthroline (35 mg, 0.195 mmol) was added and the mixture was refluxed for 1 hour. The solvent was removed in vacuo and the residue was purified by column chromatography (silica gel, CH_2Cl_2) affording the product as yellow solid. Yield 70.8 %. ^{1}H NMR (400 MHz, THF-d_8): 8.95 (s (br), 2H, Phen.), 8.67 (dd, 2H, J = 8.0, 1.6 Hz, Phen.), 8.11 (s, 2H, Phen.), 7.97 (m, 2H, Phen.), 7.77 (m, 4H, Ph), 7.39 (m, 4H, Ph), 7.20 (m, 8H, Ph), 7.13 (m, 4H, Ph), 0.75 (br, 10H, B-H). ^{31}P{H} NMR (162 MHz, THF-d_8): 19.2 ppm (dd, J = 343.9, 24.8 Hz). Calculated for $C_{38}H_{38}B_9N_2P_2Ag{\cdot}0.5CH_2Cl_2$, %: C, 55.56; H, 4.72; N, 3.37. Found, %: C, 55.60; H 4.77; N, 3.11.

Ag(idmp)(P_2-nCB). To a solution of $AgBF_4$ (75 mg, 0.385 mmol) in ethanol *bis*-(diphenylphosphine)-*ortho*-carborane (194 mg, 0.385 mmol) was added and the mixture was stirred at room temperature for 1 hour. Then 4,7-dimethyl-1,10-phenanthroline (80 mg, 0.385 mmol) was added and the mixture was refluxed for 1 hour. The solvent was removed in vacuo and the residue was purified by column chromatography (silica gel, CH_2Cl_2) affording the product as yellow solid. Yield 68.9 %. ^{1}H NMR (400 MHz, CD_2Cl_2): 8.74 (d, 2H, J = 4.0 Hz, Phen.), 8.21 (s, 2H, Phen.), 7.78-7.66 (m, 6H, Phen. and Ph), 7.37 (m, 4H, Ph), 7.30-7.15 (m, 12H, Ph), 2.9 (s, 6H, $2CH_3$), 0.75 (br, 10H, B-H). ^{31}P{H} NMR (162 MHz, CD_2Cl_2): 17.8 ppm (dd, J = 340.8, 24.3 Hz). Calculated for $C_{40}H_{42}B_9N_2P_2Ag{\cdot}0.5CH_2Cl_2$, %: C, 56.54; H, 5.04; N, 3.26. Found, %: C, 56.54; H 5.12; N, 3.13.

Ag(dmp)(P_2-nCB). To a solution of $AgPF_6$ (0.6 g, 2.4 mmol) in ethanol *bis*-(diphenylphosphine)-*ortho*-carborane (1.23 g, 2.4 mmol) was added and the mixture was stirred at room temperature for 1 hour. Then 2,9-dimethyl-1,10-phenanthroline (0.5 g, 2.4 mmol) was added and the mixture was refluxed for 1 hour. The solvent was removed in vacuo and the residue was purified by column chromatography (silica gel, CH_2Cl_2) affording the product as yellow solid. Yield 71.4 %. ^{1}H NMR (400 MHz, CD_2Cl_2): 8.35 (m, 3H, Phen.), 7.85 (m, 3H, Phen.), 7.60-7.48 (m, 8H, Phen. and Ph), 7.39-7.25 (m, 12H, Ph), 1.27 (s, 6H, $2CH_3$), 0.75 (br, 10H, B-H). ^{31}P{H} NMR (162 MHz, CD_2Cl_2): 18.5 ppm (dd, J = 335.0, 23.9 Hz). Calculated for $C_{40}H_{42}B_9N_2P_2Ag$, %: C, 58.74; H, 5.18; N, 3.43. Found, %: C, 58.51; H 5.13; N, 3.48.

Ag(dbp)(P_2-nCB). To a solution of $AgPF_6$ (0.6 g, 2.4 mmol) in ethanol *bis*-(diphenylphosphine)-*ortho*-carborane (1.2 g, 2.4 mmol) was added and the mixture was stirred at room temperature for 1 hour. Then 2,9-di-*n*-butyl-1,10-phenanthroline (0.7 g, 2.4 mmol) was added and the mixture was refluxed for 1 hour. The solvent was removed in vacuo and the residue was purified by column chromatography (silica gel, CH_2Cl_2) affording the product as a yellow solid. Yield 68.8 %. ^{1}H NMR (DMSO-d_6): 8.78 (d, 2H, J = 8.17, Phen.), 8.21 (s, 2H, Phen.), 8.02 (d, 2H, J = 8.60, Phen.), 6.80-7.50 (m, 20H, $P(Ph)_2$), 4.02(m, 2H, n-Bu), 1.51(m, 8H, n-Bu), 0.75 (br, 10H, B-H), 0.21(m, 8H, n-Bu). ^{31}P{H} NMR (162 MHz, DMSO-d_6): 20.9 ppm (dd, J = 245.9, 17.6 Hz). Calculated for $C_{46}H_{54}B_9N_2P_2Ag$, %: C, 61.25; H, 6.03; N, 3.11. Found, %: C, 60.98; H, 5.97; N, 2.95.

Photophysics.

Photophysical measurements were performed for a powder sample deposited in a helium cryostat (Cryovac Konti Cryostat IT) in which the helium gas flow, gas pressure, and heating were controlled. Thus, the temperature was varied between 1.5 and 300 K. Luminescence spectra were measured with a Horiba Jobin Yvon Fluorolog 3 steady-state fluorescence spectrometer. This spectrometer was modified to allow for measurements of emission decay times. As excitation source a PicoBright PB-375 pulsed diode laser (λ_{exc} =

378 nm, pulse width 100 ps) was used. The emission signal was detected with a cooled photomultiplier attached to a FAST ComTec multichannel scalar PCI card with a time resolution of 250 ps. Photoluminescence quantum yields were determined with a Hamamatsu C9920-02 system equipped with a Spectralon® integrating sphere.

X-ray diffraction studies.

Ag(phen)(P_2-nCB). A clear yellow prism-shaped crystal with dimensions 0.35×0.17×0.13 was mounted on a MITIGEN holder with inert grease. Data were collected using a SuperNova, Single source at offset, Atlas diffractometer equipped with an Oxford Cryosystems CryoStream 700 low-temperature apparatus operating at T = 123 K. Data were measured using scans of 1.0° per frame for 1.0 s using CuK_a radiation (micro-focus sealed X-ray tube). The total number of runs and images was based on the strategy calculation from the program CrysAlisPro (Agilent). The actually achieved resolution was Q = 76.462.

Cell parameters were retrieved using the CrysAlisPro (Agilent) software and refined using CrysAlisPro (Agilent) on 14071 reflections, 59 of the observed reflections. Data reduction was performed using the CrysAlisPro (Agilent) software which corrects for Lorentz polarization. The final completeness is 99.90 out to 76.462 in Q. The absorption coefficient (m) of this material is 5.496 and the minimum and maximum transmissions are 0.750 and 0.885.

The structure was solved in the space group $P2_1/n$ (# 14) by Direct Methods using the ShelXT (Sheldrick, 2015) structure solution program and refined by Least Squares using ShelXL (Sheldrick, 2015). All non-hydrogen atoms were refined anizotropically. Hydrogen atom positions were calculated geometrically and refined using the riding model.

Ag(idmp)(P_2-nCB). A clear light-yellow plate-shaped crystal with dimensions 0.32×0.12×0.04 was mounted on a MITIGEN holder with inert oil. Data were collected using a SuperNova, Single source at offset, Atlas diffractometer equipped with an Oxford Cryosystems CryoStream 700 low-temperature apparatus operating at T = 123 K. Data were measured using scans scans of 1.0° per frame for 2.5 s using CuK_a radiation (micro-focus sealed X-ray tube). The total number of runs and images was based on the strategy calculation from the program CrysAlisPro (Agilent). The actually achieved resolution was Q = 76.406.

Cell parameters were retrieved using the CrysAlisPro (Agilent) software and refined using CrysAlisPro (Agilent) on 27103 reflections, 45 of the observed reflections. Data reduction was performed using the CrysAlisPro (Agilent) software which corrects for Lorentz polarization. The final completeness is 100.00 out to 76.406 in Q. The absorption coefficient (m) of this material is 5.243 and the minimum and maximum transmissions are 0.887 and 0.975.

The structure was solved in the space group Pbca (# 61) by Direct Methods using the ShelXT (Sheldrick, 2015) structure solution program and refined by Least Squares using ShelXL (Sheldrick, 2015). All non-hydrogen atoms were refined anisotropically. Hydrogen atom positions were calculated geometrically and refined using the riding model.

Ag(dmp)(P_2-nCB). A clear colorless irregular-shaped crystal with dimensions 0.17×0.11×0.05 was mounted on a MITIGEN holder with inert oil. Data were collected using a SuperNova, Single source at offset, Atlas diffractometer equipped with an Oxford Cryosystems CryoStream 700 low-temperature apparatus operating at T = 123 K.

Data were measured using scans of 1.0° per frame for 2.0 s using CuK_a radiation (micro-focus sealed X-ray tube). The total number of runs and images was based on the strategy calculation from the program CrysAlisPro (Agilent). The actually achieved resolution was Q = 73.608.

Cell parameters were retrieved using the CrysAlisPro (Agilent) software and refined using CrysAlisPro (Agilent) on 7720 reflections, 48 of the observed reflections. Data reduction was performed using the CrysAlisPro (Agilent) software which corrects for Lorentz polarization. The final completeness is 98.50 out to 73.608 in Q. The absorption coefficient (m) of this material is 5.958 and the minimum and maximum transmissions are 0.798 and 0.909.

The structure was solved in the space group P-1 (# 2) by Direct Methods using the ShelXT (Sheldrick, 2015) structure solution program and refined by Least Squares using ShelXL (Sheldrick, 2015). All non-hydrogen atoms were refined anizotropically. Hydrogen atom positions were calculated geometrically and refined using the riding model.

Ag(dbp)(P_2-nCB). A light-yellow plate-shaped crystal with dimensions 0.21×0.12×0.08 mm^3 was mounted on a MITIGEN holder with inert oil. X-ray diffraction data were collected using a SuperNova, Single source at offset, Atlas diffractometer equipped with an Oxford Cryosystems CryoStream 700 low-temperature device, operating at T = 123 K.

Data were measured using w scans of 0.5 ° per frame for 10.0 s using CuK_a radiation (micro-focus sealed X-ray tube). The total number of runs and images was based on the strategy calculation from the program CrysAlisPro (Agilent). The maximum resolution achieved was Q = 73.484

Cell parameters were retrieved using the CrysAlisPro (Agilent) software and refined using CrysAlisPro (Agilent) on 35923 reflections, 60 % of the observed reflections. Data reduction was performed using the CrysAlisPro (Agilent) software which corrects for Lorentz polarization. The final completeness is 99.30 out to 73.484 in Q. The absorption coefficient m of this material is 4.089 at this wavelength (l = 1.54184) and the minimum and maximum transmissions are 0.928 and 0.976.

The structure was solved in the space group $P2_1/c$ (# 14) Direct Methods using the ShelXT 2014/5 (Sheldrick, 2014) structure solution program and refined by Least Squares using version 2014/7 of **ShelXL** (Sheldrick, 2015). All non-hydrogen atoms were refined anizotropically. Hydrogen atom positions were calculated geometrically and refined using the riding model.

Table S1. Crystal data, data collection, and structure refinement details.

Compound	**Ag(phen)(P_2-nCB)**	**Ag(idmp)(P_2-nCB)**	**Ag(dmp)(P_2-nCB)**	**Ag(dbp)(P_2-nCB)**
Formula	$C_{38}H_{38}AgB_9N_2P_2$	$C_{40}H_{42}AgB_9N_2P_2$	$C_{41}H_{44}AgB_9Cl_2N_2P_2$	$C_{96}H_{118}Ag_2B_{18}N_4OP_4$
$D_{calc.}$/ g cm^{-3}	1.438	1.415	1.421	1.246
m/mm^{-1}	5.496	5.243	5.958	4.089
Formula Weight	789.80	817.85	902.78	1878.14
Colour	clear yellow	clear light yellow	clear colorless	light yellow
Shape	prism	plate	irregular	plate
Max Size/mm	0.35	0.32	0.17	0.21
Mid Size/mm	0.17	0.12	0.11	0.12
Min Size/mm	0.13	0.04	0.05	0.08
T/K	123	123	123	293.53(10)
Crystal System	monoclinic	orthorhombic	triclinic	monoclinic
Space Group	$P2_1/n$	Pbca	P-1	$P2_1/c$
a/Å	15.45090(17)	13.84462(16)	10.9528(4)	18.24578(12)
b/Å	13.73540(18)	22.8202(3)	13.8545(5)	23.5847(2)
c/Å	17.2173(2)	24.2963(2)	15.6337(7)	23.60800(17)
a/°	90	90	67.617(4)	90
b/°	93.3473(11)	90	82.186(4)	99.6853(7)
g/°	90	90	74.331(4)	90
V/Å^3	3647.70(8)	7676.07(15)	2110.61(17)	10014.25(13)
Z	4	8	2	4
Z'	1	1	1	1
Q_{min}/°	3.737	3.638	3.553	3.404
Q_{max}/°	76.462	76.406	73.608	73.484
Measured Refl.	23813	60763	16213	59570
Independent Refl.	7610	8029	8086	19465
Reflections Used	7095	7309	7115	17850
R_{int}	0.0275	0.0353	0.0372	0.0242
Parameters	485	505	556	1180
Restraints	0	0	1	3
Largest Peak	1.001	3.137	0.458	0.862
Deepest Hole	-0.762	-1.425	-0.707	-0.754
GooF	1.033	1.036	1.029	1.019
wR_2 (all data)	0.0658	0.1122	0.0807	0.0854
wR_2	0.0642	0.1086	0.0771	0.0830
R_1 (all data)	0.0279	0.0429	0.0378	0.0330
R_1	0.0254	0.0393	0.0312	0.0298

Table S2. Coordination center geometry parameters of complexes Ag(phen)(P_2-nCB), Ag(idmp)(P_2-nCB), Ag(dmp)(P_2-nCB), Ag(dbp)(P_2-nCB) obtained by single crystal X-ray diffraction analyses. Atom numbering corresponds to the one shown in Figure 2.

Parameters	Ag(phen)(P_2-nCB)	Ag(idmp)(P_2-nCB)	Ag(dmp)(P_2-nCB)	Ag(dbp)(P_2-nCB)
		Bonds (Å)		
Ag-N1	2.3010(16)	2.281(2)	2.329(2)	2.3158(18)
Ag-N2	2.4013(16)	2.339(2)	2.348(3)	2.3207(16)
Ag-P1	2.4908(4)	2.4666(6)	2.4816(6)	2.4230(5)
Ag-P2	2.4617(4)	2.4531(7)	2.4395(6)	2.4770(5)
		Angles (degree^o)		
N1-Ag-P1	146.08(4)	141.29(6)	118.56(5)	133.87(4)
N1-Ag-P2	122.11(4)	122.37(6)	137.84(5)	120.64(4)
N2-Ag-P1	114.27(4)	118.98(6)	109.63(5)	132.29(4)
N2-Ag-P2	126.20(4)	125.31(6)	133.91(6)	115.99(4)
N1-Ag-N2	71.78(5)	71.75(8)	72.32(8)	72.99(6)
P1-Ag-P2	82.670(14)	83.49(2)	86.443(19)	85.581(16)
		Dihedral angles (degree^o)		
C1-N1-Ag-P1	77.88(17)	66.8(3)	77.0(2)	44.34(18)
C1-N1-Ag-P2	53.67(16)	58.4(2)	42.7(2)	72.10(16)
C2-N2-Ag-P1	31.77(17)	34.7(3)	65.1(2)	41.87(19)
C2-N2-Ag-P2	67.24(16)	68.8(2)	39.5(3)	67.26(17)

Calculations.

M06[1]/def2-SVP[2,3] level of theory with "tight" criteria was applied for geometry optimizations and M062X[1]/def2-SVP level of theory was applied for time-dependent calculations, all using the Gaussian 09D[4] program.

Table S3. Coordination center geometry parameters of complexes Ag(phen)(P_2-nCB), Ag(idmp)(P_2-nCB), Ag(dmp)(P_2-nCB), Ag(dbp)(P_2-nCB) calculated (M06/def2-SVP) for ground state (S_0) in gas phase conditions. Atom numbering corresponds to the one shown in Figure 2.

Parameters	Ag(phen)(P_2-nCB)	Ag(idmp)(P_2-nCB)	Ag(dmp)(P_2-nCB)	Ag(dbp)(P_2-nCB)
		Bonds (Å)		
Ag-N1	2.34229	2.34115	2.41179	2.35801
Ag-N2	2.45112	2.43338	2.39121	2.39355
Ag-P1	2.50645	2.50418	2.55064	2.49284
Ag-P2	2.56270	2.56886	2.54173	2.54347
		Angles (degree^o)		
N1-Ag-P1	152.825	153.231	132.799	134.906
N1-Ag-P2	124.275	123.772	133.785	120.787
N2-Ag-P1	109.467	110.866	118.905	132.180
N2-Ag-P2	115.100	114.829	125.552	118.865
N1-Ag-N2	70.372	69.959	70.538	71.021
P1-Ag-P2	81.286	81.140	81.365	84.466
		Dihedral angles (degree^o)		
C1-N1-Ag-P1	85.451	83.088	69.467	49.676
C1-N1-Ag-P2	72.383	73.012	57.696	66.131
C2-N2-Ag-P1	27.626	27.482	51.068	47.207
C2-N2-Ag-P2	61.693	62.218	49.523	63.335

Table S4. Coordination center geometry parameters of complexes Ag(phen)(P_2-nCB), Ag(idmp)(P_2-nCB), Ag(dmp)(P_2-nCB), Ag(dbp)(P_2-nCB) calculated (M06/def2-SVP) for the lowest excited triplet state (T_1) in gas phase conditions. Atom numbering corresponds to the one shown in Figure 2.

Parameters	Ag(phen)(P_2-nCB)	Ag(idmp)(P_2-nCB)	Ag(dmp)(P_2-nCB)	Ag(dbp)(P_2-nCB)
		Bonds (Å)		
Ag-N1	2.18688	2.17041	2.19366	2.18167
Ag-N2	2.25457	2.26144	2.35313	2.36246
Ag-P1	2.46402	2.45937	2.42415	2.43739
Ag-P2	2.53833	2.54136	2.64561	2.59068
		Angles (degree^o)		
N1-Ag-P1	170.531	171.368	161.166	155.147
N1-Ag-P2	98.932	98.930	101.706	106.467
N2-Ag-P1	110.947	110.928	122.576	124.317
N2-Ag-P2	139.305	137.861	106.577	113.240
N1-Ag-N2	76.915	76.419	75.254	75.557
P1-Ag-P2	78.651	78.759	80.006	80.646
		Dihedral angles (degree^o)		
C1-N1-Ag-P1	35.415	33.406	9.598	29.651
C1-N1-Ag-P2	39.009	40.359	83.756	73.933
C2-N2-Ag-P1	10.189	8.962	5.870	22.890
C2-N2-Ag-P2	86.817	87.445	82.716	71.638

Table S5. Excited state properties of Ag(phen)(P_2-nCB) obtained from TD-DFT calculations (M062X/Def2-SVP) for the gas phase relaxed geometry of the lowest excited triplet state (T_1).

State	Energy (eV)	Main contributions	Oscillator strength	Character
S_1	1.73	HOMO → LUMO (92%), HOMO−1→ LUMO (4%)	0.0258	$^1(ML_{P2\text{-}nCB})L_{phen}CT$
S_2	2.36	HOMO → LUMO+1 (94%), HOMO−1→ LUMO+1 (3%)	0.0015	$^1(ML_{P2\text{-}nCB})L_{phen}CT$
S_3	3.06	HOMO → LUMO (5%), HOMO−1→ LUMO (92%)	0.0002	$^1(ML_{P2\text{-}nCB})L_{phen}CT$
S_8	3.83	HOMO−2 → LUMO (45%), HOMO → LUMO+4 (10%), HOMO−19 → LUMO (6%), HOMO−4 → LUMO (6%), HOMO−14 → LUMO (5%).	0.0149	$^1(ML_{P2\text{-}nCB})L_{phen}CT$
T_1	1.59	HOMO → LUMO (89%), HOMO−1→ LUMO (4%)	0	$^3(ML_{P2\text{-}nCB})L_{phen}CT$
T_2	2.31	HOMO → LUMO+1 (92%), HOMO−1→ LUMO+1 (3%).	0	$^3(ML_{P2\text{-}nCB})L_{phen}CT$
T_3	3.04	HOMO → LUMO (7%), HOMO−1→ LUMO (88%)	0	$^3(ML_{P2\text{-}nCB})L_{phen}CT$

Table S6. Excited state properties of Ag(idmp)(P_2-nCB) obtained from TD-DFT calculations (M062X/Def2-SVP) for the gas phase relaxed geometry of the lowest excited triplet state (T_1).

State	Energy (eV)	Main contributions	Oscillator strength	Character
S_1	1.87	HOMO → LUMO (89%), HOMO−1→ LUMO (3%), HOMO→ LUMO+1 (3%).	0.0270	$^1(ML_{P2\text{-}nCB})L_{idmp}CT$
S_2	2.33	HOMO → LUMO (3%), HOMO−1→ LUMO (91%).	0.0200	$^1(ML_{P2\text{-}nCB})L_{idmp}CT$
S_3	3.24	HOMO → LUMO (5%), HOMO−1 → LUMO+1 (4%), HOMO−1→ LUMO (88%).	0.0002	$^1(ML_{P2\text{-}nCB})L_{idmp}CT$
S_8	3.91	HOMO → LUMO+5 (23%), HOMO → LUMO+4 (18%), HOMO → LUMO+7 (14%), HOMO−2 → LUMO (9%), HOMO → LUMO+6 (5%).	0.0465	$^1IL_{P2\text{-}nCB}CT$
S_9	4.00	HOMO−2 → LUMO (43%), HOMO → LUMO+5 (13%), HOMO → LUMO+6 (6%), HOMO−4 → LUMO (5%), HOMO−13 → LUMO (4%).	0.0351	$^1(ML_{P2\text{-}nCB})L_{idmp}CT$
T_1	1.74	HOMO → LUMO (85%), HOMO−1→ LUMO (4%), HOMO→ LUMO+2 (3%).	0	$^3(ML_{P2\text{-}nCB})L_{idmp}CT$
T_2	2.28	HOMO → LUMO+1 (89%), HOMO → LUMO (3%), HOMO−1 → LUMO+1 (2%).	0	$^3(ML_{P2\text{-}nCB})L_{idmp}CT$
T_3	3.10	HOMO−16 → LUMO (17%), HOMO−10 → LUMO (16%), HOMO−10 → LUMO+1 (12%), HOMO−13 → LUMO+1 (8%), HOMO−11 → LUMO+1 (6%), HOMO−11 → LUMO (5%), HOMO−13 → LUMO (4%), HOMO−16 → LUMO+1 (3%), HOMO−15 → LUMO (3%).	0	$^3IL_{idmp}CT$

Table S7. Excited state properties of Ag(dmp)(P_2-nCB) obtained from TD-DFT calculations (M062X/Def2-SVP) for the gas phase relaxed geometry of the lowest excited triplet state (T_1).

State	Energy (eV)	Main contributions	Oscillator strength	Character
S_1	2.17	HOMO → LUMO (96 %).	0.0423	$^1(ML_{P2\text{-}nCB})L_{dmp}CT$
S_2	2.80	HOMO → LUMO+1 (97%).	0.0058	$^1(ML_{P2\text{-}nCB})L_{dmp}CT$
S_3	3.28	HOMO−1 → LUMO (96%), HOMO→ LUMO (2%).	0.0002	$^1(L_{P2\text{-}nCB})L_{dmp}CT$
S_4	3.66	HOMO−2 → LUMO (39%), HOMO−14 → LUMO (11%), HOMO−8 → LUMO (10%), HOMO−17 → LUMO (8%), HOMO−4 → LUMO (7%), HOMO−13 → LUMO (5%).	0.0050	$^1(ML_{P2\text{-}nCB})L_{dmp}CT$
T_1	2.04	HOMO → LUMO (94 %), HOMO−1 → LUMO (2 %).	0	$^3(ML_{P2\text{-}nCB})L_{dmp}CT$
T_2	2.74	HOMO → LUMO+1 (92 %), HOMO−8 → LUMO+1 (2 %).	0	$^3(ML_{P2\text{-}nCB})L_{dmp}CT$
T_3	3.15	HOMO−9 → LUMO (23%), HOMO−9 → LUMO+1 (14%), HOMO−15 → LUMO (13%), HOMO−16 → LUMO (6%), HOMO−6 → LUMO (5%)	0	$^3IL_{dmp}CT$

Table S8. Excited state properties of Ag(dbp)(P_2-nCB) obtained from TD-DFT calculations (M062X/Def2-SVP) for the gas phase relaxed geometry of the lowest excited triplet state (T_1).

State	Energy (eV)	Main contributions	Oscillator strength	Character
S_1	2.36	HOMO → LUMO (92 %), HOMO−1 → LUMO (4 %).	0.0536	$^1(ML_{P2\text{-}nCB})L_{dbp}CT$
S_2	2.99	HOMO → LUMO+1 (95 %), HOMO−1 → LUMO+1 (3 %).	0.0066	$^1(ML_{P2\text{-}nCB})L_{dbp}CT$
S_3	3.36	HOMO → LUMO (4 %), HOMO−1 → LUMO (94 %)	0.0004	$^1(L_{P2\text{-}nCB})L_{dbp}CT$
S_4	3.77	HOMO−2 → LUMO (33 %), HOMO−2 → LUMO (20 %), HOMO−17 → LUMO (9 %), HOMO−9 → LUMO (5 %), HOMO−5 → LUMO (3 %).	0.0104	$^1(ML_{P2\text{-}nCB})L_{dbp}CT$
T_1	2.21	HOMO → LUMO (90%), HOMO−1 → LUMO (4%)	0	$^3(ML_{P2\text{-}nCB})L_{dbp}CT$
T_2	2.91	HOMO → LUMO+1 (79 %), HOMO−1 → LUMO+1 (3 %), HOMO−9 → LUMO+1 (2 %).	0	$^3(ML_{P2\text{-}nCB})L_{dbp}CT$
T_3	3.17	HOMO → LUMO+1 (10 %), HOMO−7 → LUMO (6 %), HOMO−8 → LUMO (5 %), HOMO−9 → LUMO+1 (7 %), HOMO−9 → LUMO (17 %), HOMO−10 → LUMO (3 %), HOMO−15 → LUMO (14 %), HOMO−11 → LUMO (6 %).	0	$^3(L_{P2\text{-}nCB})L_{dbp}CT$

Table S9. Orbital energies and compositions of Ag(phen)(P_2-nCB) resulting from Mulliken population analysis at the M062X/def2-SVP level of theory in the gas phase relaxed geometry of the lowest excited triplet state (T_1).

Orbital	Energy, (eV)	Contributions, (%)				
		phen [a]	Ag	P	Ph. [b]	nCB [c]
LUMO+4	0.03	1	7	8	81	3
LUMO+3	-0.25	0	2	12	82	3
LUMO+2	-0.50	92	4	1	3	0
LUMO+1	-1.81	100	0	0	0	0
LUMO	-2.22	96	2	1	1	0
HOMO	-5.77	6	15	45	13	20
HOMO−1	-6.56	1	3	10	4	82
HOMO−2	-7.69	2	9	21	24	44
HOMO−3	-7.93	0	1	2	53	44
HOMO−4	-8.11	2	2	1	33	62

a) phenanthroline ligand (phen)
b) phenyl groups of P_2-nCB ligand
c) *nido*-carboranyl moiety of P_2-nCB ligand

Table S10. Orbital energies and compositions of Ag(idmp)(P_2-nCB) resulting from Mulliken population analysis at the M062X/def2-SVP level of theory in the gas phase relaxed geometry of the lowest excited triplet state (T_1).

Orbital	Energy, (eV)	Contributions, (%)				
		idmp [a]	Ag	P	Ph. [b]	nCB [c]
LUMO+4	-0.08	1	7	8	81	3
LUMO+3	-0.20	0	2	12	82	3
LUMO+2	-0.38	91	4	1	4	0
LUMO+1	-1.77	99	1	0	0	0
LUMO	-2.02	96	2	1	1	0
HOMO	-5.70	6	16	45	13	19
HOMO−1	-6.50	1	3	9	4	83
HOMO−2	-7.63	2	9	22	24	42
HOMO−3	-7.88	0	1	2	53	44
HOMO−4	-8.06	3	2	1	34	60

a) 4,7-di-methyl-phenanthroline ligand (idmp)
b) phenyl groups of P_2-nCB ligand
c) *nido*-carboranyl moiety of P_2-nCB ligand

Table S11. Orbital energies and compositions of Ag(dmp)(P_2-nCB) resulting from Mulliken population analysis at the M062X/def2-SVP level of theory in the gas phase relaxed geometry of the lowest excited triplet state (T_1).

Orbital	Energy, (eV)	Contributions, (%)				
		dmp [a]	Ag	P	Ph. [b]	nCB [c]
LUMO+4	-0.06	12	1	8	77	2
LUMO+3	-0.13	4	2	9	80	4
LUMO+2	-0.43	78	6	2	14	1
LUMO+1	-1.65	99	0	0	1	0
LUMO	-2.14	96	2	1	1	0
HOMO	-5.99	3	12	49	23	13
HOMO−1	-6.58	0	1	5	4	90
HOMO−2	-7.67	3	11	23	31	32
HOMO−3	-8.00	1	1	1	29	68
HOMO−4	-8.20	4	4	3	33	56

a) 2,9-di-methyl-phenanthroline ligand (dmp)
b) phenyl groups of P_2-nCB ligand
c) *nido*-carboranyl moiety of P_2-nCB ligand

Table S12. Orbital energies and compositions of Ag(dbp)(P_2-nCB) resulting from Mulliken population analysis at the M062X/def2-SVP level of theory in the gas phase relaxed geometry of the lowest excited triplet state (T_1).

Orbital	Energy, (eV)	Contributions, (%)				
		dbp [a]	Ag	P	Ph. [b]	nCB [c]
LUMO+4	0.04	3	2	9	84	2
LUMO+3	-0.16	4	4	9	81	3
LUMO+2	-0.35	87	4	1	5	0
LUMO+1	-1.61	92	0	0	0	0
LUMO	-2.09	90	1	1	1	0
HOMO	-6.09	3	13	47	18	16
HOMO−1	-6.60	1	2	8	5	76
HOMO−2	-7.65	2	10	23	33	28
HOMO−3	-8.02	1	0	1	42	54
HOMO−4	-8.12	1	1	1	34	59

a) 2,9-di-*n*-butyl-phenanthroline ligand (dbp)
b) phenyl groups of P_2-nCB ligand
c) *nido*-carboranyl moiety of P_2-nCB ligand

Figure S1. Iso-surface contour plots (iso-value 0.05) and energies of the molecular orbital relevant to the lowest excited states of Ag(phen)(P_2-nCB) as calculated at the M062X/def2-SVP theory level in the lowest triplet-state (T_1) geometry.

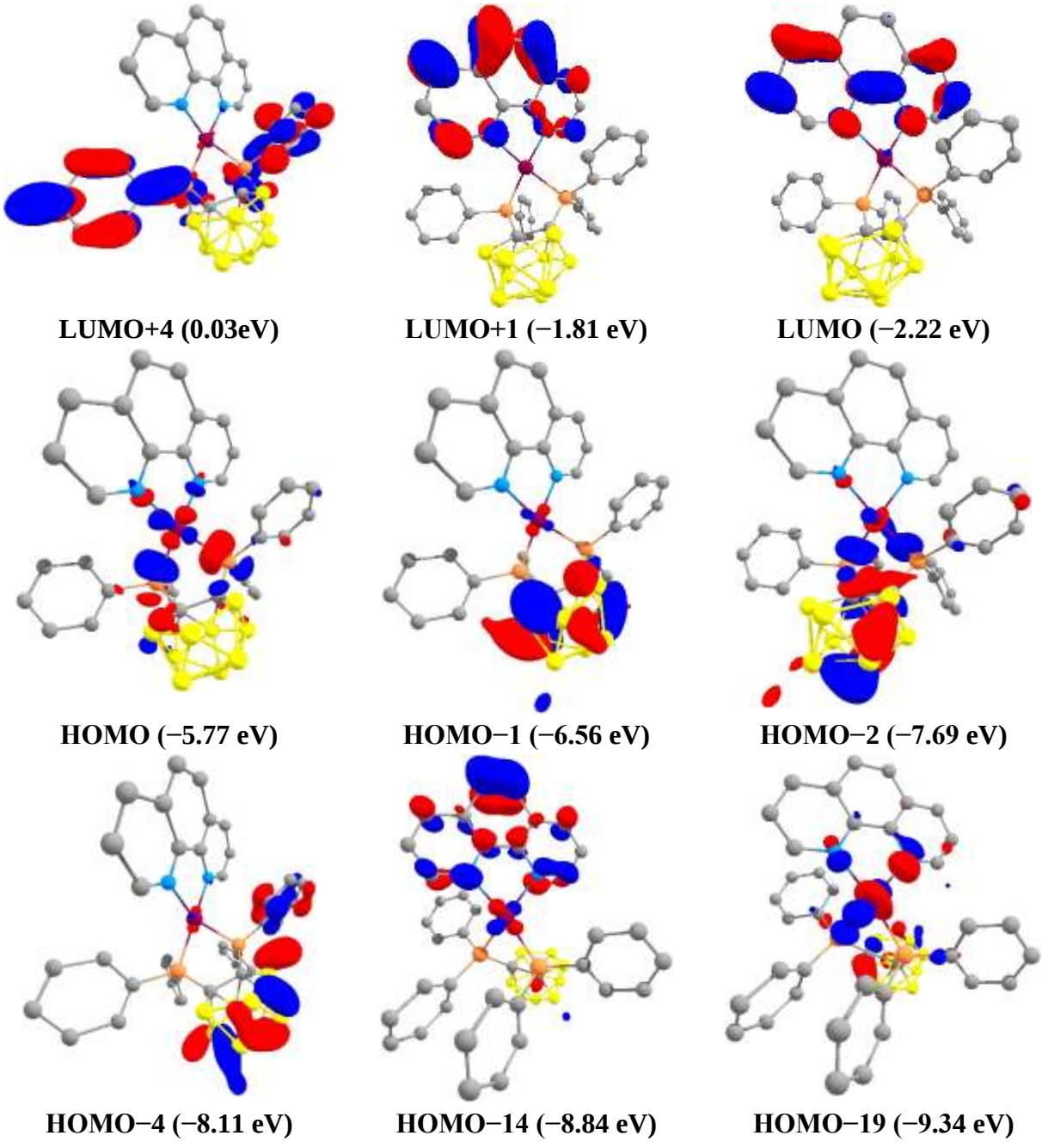

Figure S2. Iso-surface contour plots (iso-value 0.05) and energies of the molecular orbital relevant to the lowest excited states of Ag(idmp)(P_2-nCB) as calculated at the M062X/def2-SVP theory level in the lowest triplet-state (T_1) geometry.

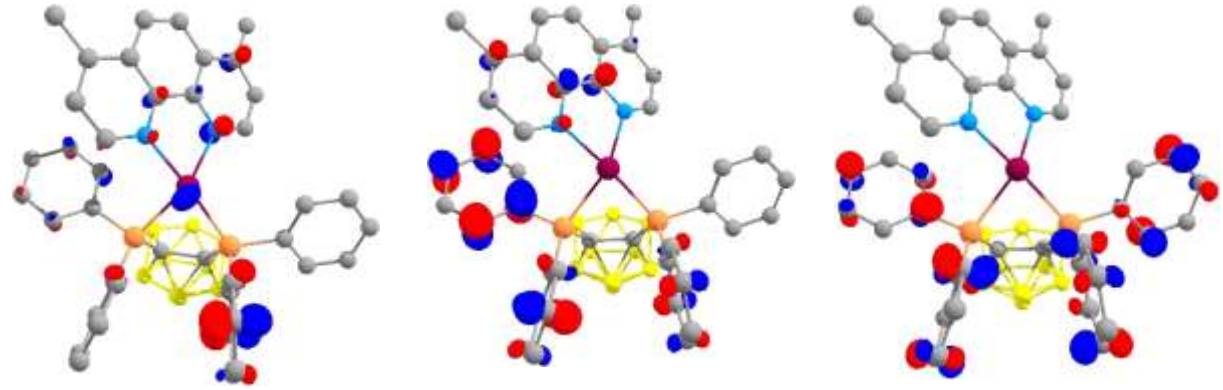

LUMO+7 (0.48 eV) **LUMO+6 (0.42 eV)** **LUMO+5 (0.29 eV)**

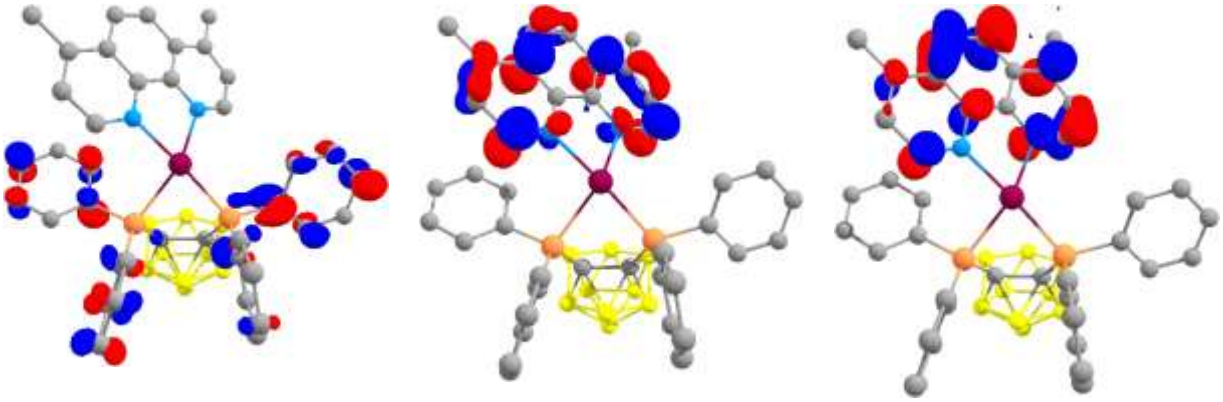

LUMO+4 (0.08 eV) **LUMO+2 (−0.38 eV)** **LUMO+1 (−1.77 eV)**

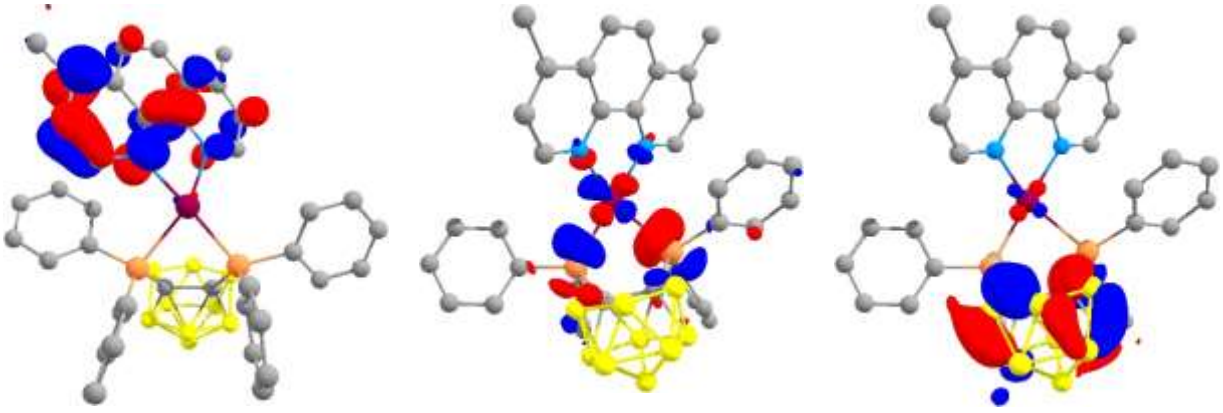

LUMO (−2.02 eV) **HOMO (−5.70 eV)** **HOMO−1 (−6.50 eV)**

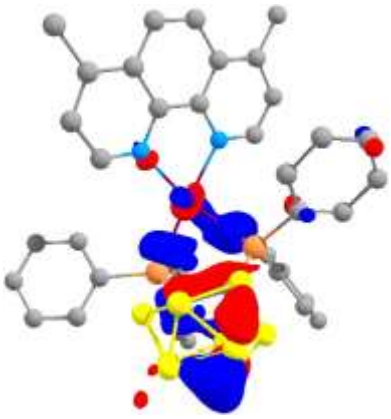

HOMO−2 (−7.63 eV)

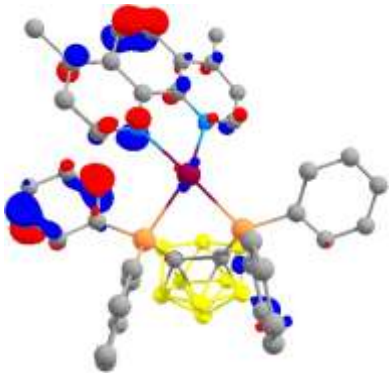

HOMO−10 (−8.47 eV)

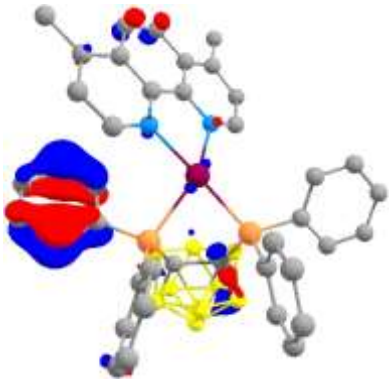

HOMO−11 (−8.53 eV)

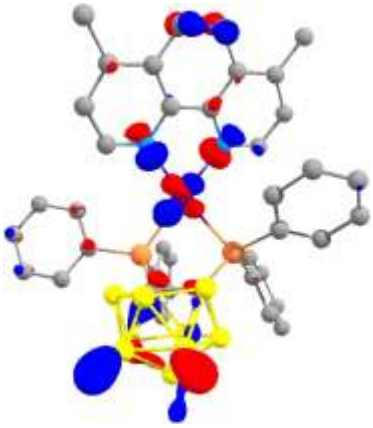

HOMO−13 (−8.66 eV)

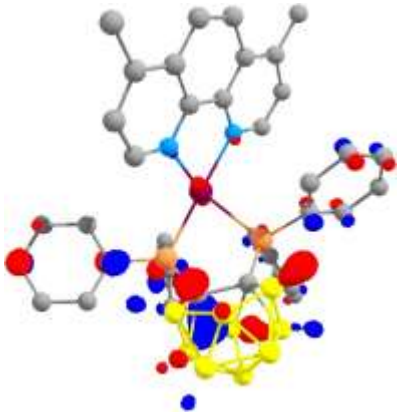

HOMO−15 (−8.88 eV)

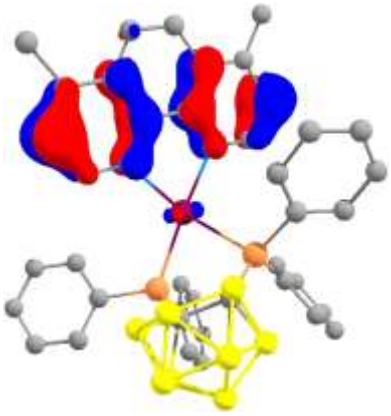

HOMO−16 (−8.91 eV)

Figure S3. Iso-surface contour plots (iso-value 0.05) and energies of the molecular orbital relevant to the lowest excited states of Ag(dmp)(P_2-nCB) as calculated at the M062X/def2-SVP theory level in the lowest triplet-state (T_1) geometry.

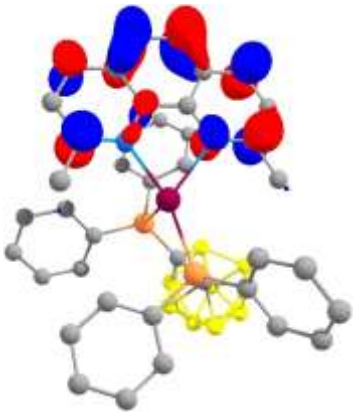

LUMO+1 (−1.65 eV)

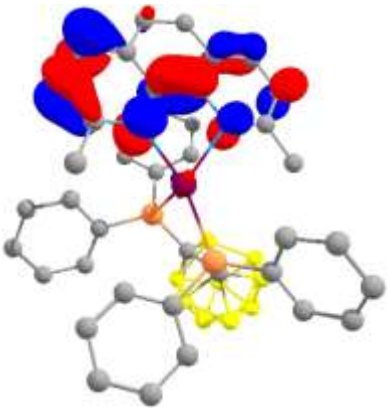

LUMO (−2.14 eV)

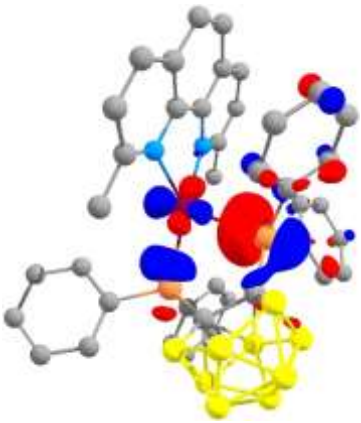

HOMO (−5.99 eV)

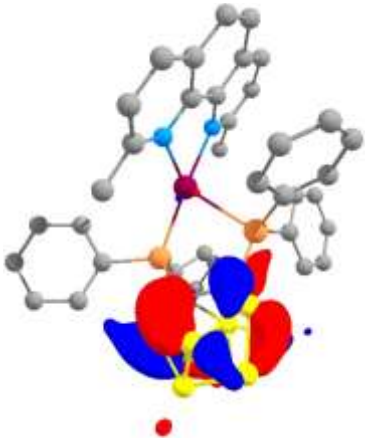

HOMO−1 (−6.58 eV)

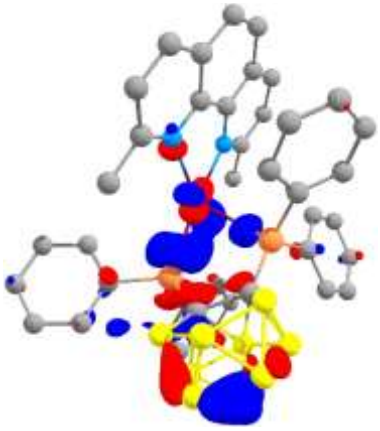

HOMO−2 (−7.67 eV)

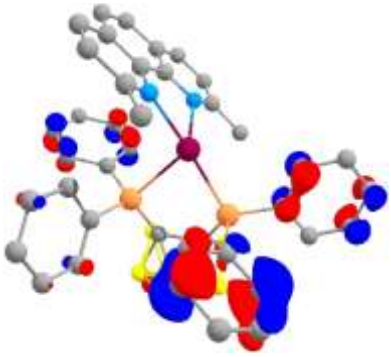

HOMO−6 (−8.33 eV)

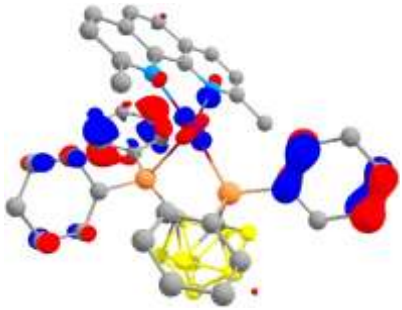

HOMO−8 (−8.47 eV)

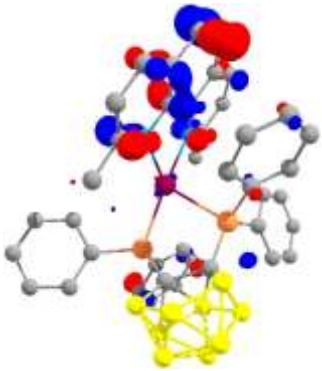

HOMO−9 (−8.48 eV)

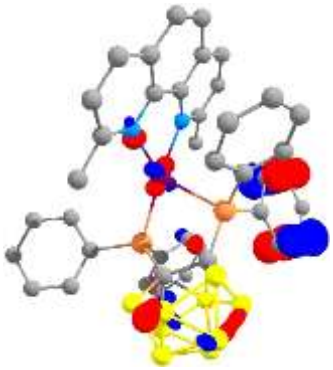

HOMO−13 (−8.74 eV)

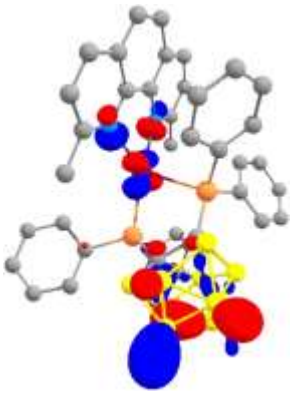

HOMO−14 (−8.81 eV)

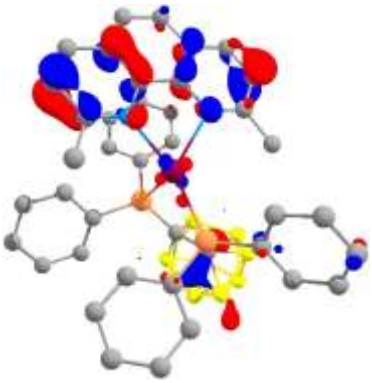

HOMO−15 (−8.91 eV)

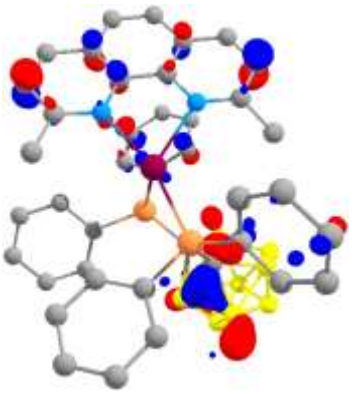

HOMO−16 (−8.93 eV)

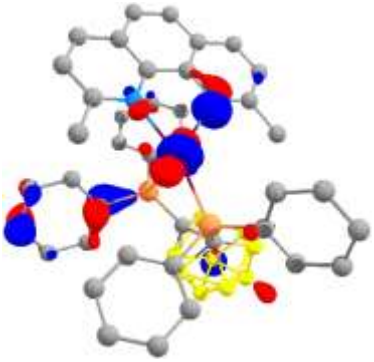

HOMO−17 (−9.15 eV)

Figure S4. Iso-surface contour plots (iso-value 0.05) and energies of the molecular orbital relevant to the lowest excited states of Ag(dbp)(P_2-nCB) as calculated at the M062X/def2-SVP theory level in the lowest triplet-state (T_1) geometry.

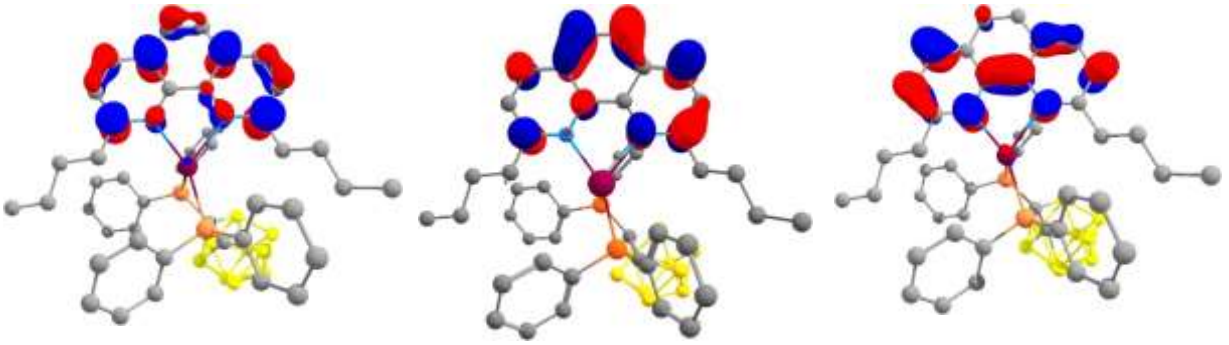

LUMO+2 (−0.35 eV) **LUMO+1 (−1.61 eV)** **LUMO (−2.09 eV)**

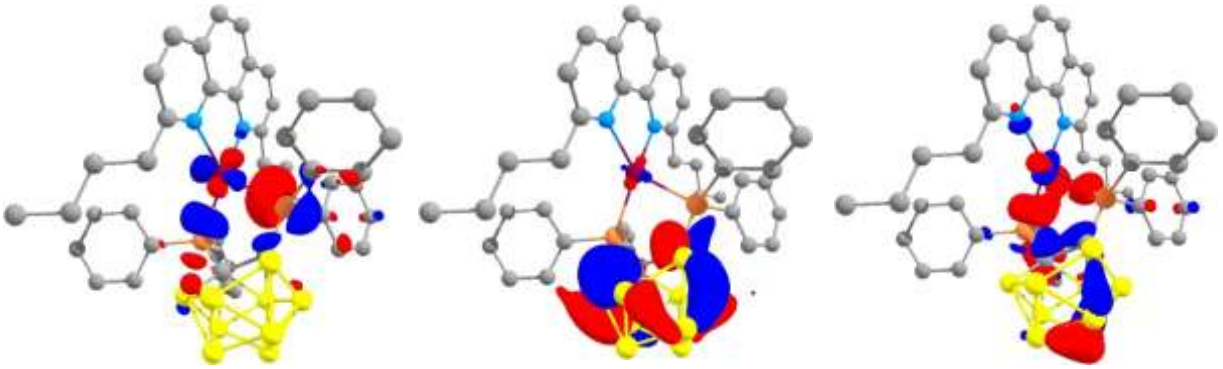

HOMO (−6.09 eV) **HOMO−1 (−6.59 eV)** **HOMO−2 (−7.65 eV)**

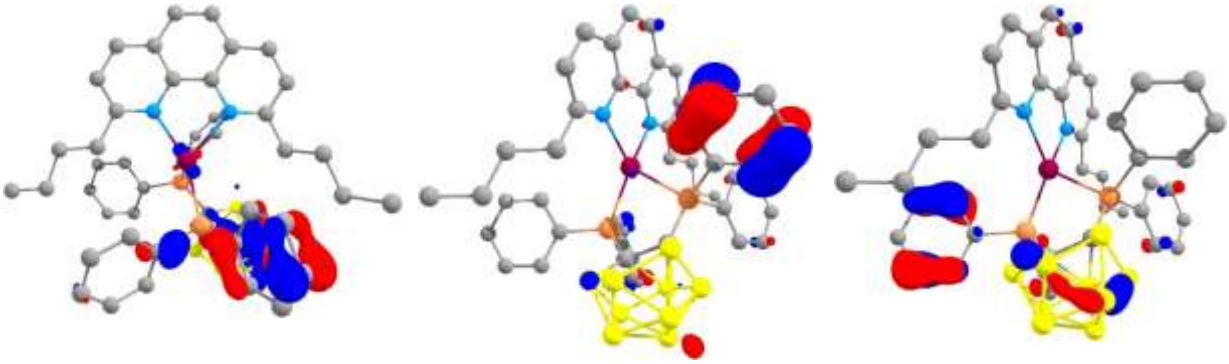

HOMO−5 (−8.28 eV) **HOMO−7 (−8.37 eV)** **HOMO−8 (−8.44 eV)**

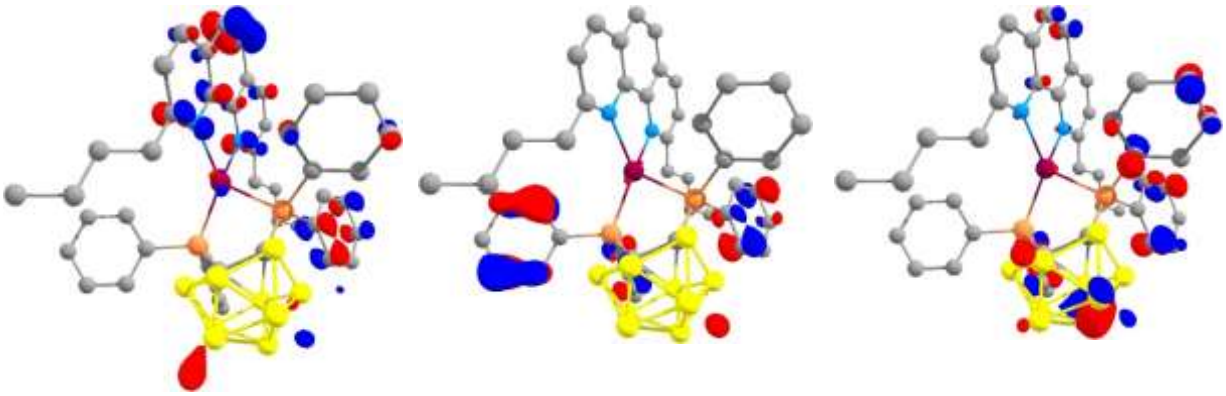

HOMO−9 (−8.47 eV) **HOMO−10 (−8.51 eV)** **HOMO−11 (−8.56 eV)**

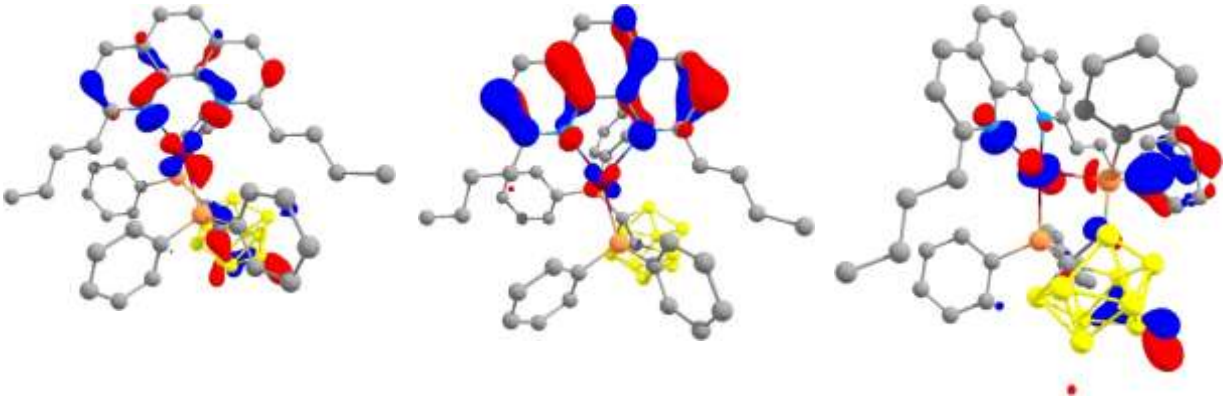

HOMO−14 (−8.79 eV) **HOMO−15 (−8.84 eV)** **HOMO−17 (−9.00 eV)**

References.

(1) Zhao, Y.; Truhlar, D. G. The M06 suite of density functionals for main group thermochemistry, thermochemical kinetics, noncovalent interactions, excited states, and transition elements: two new functionals and systematic testing of four M06-class functionals and 12 other functionals. *Theor. Chem. Acc.* **2007,** *120*, 215-241.

(2) Weigend, F.; Ahlrichs, R. Balanced basis sets of split valence, triple zeta valence and quadruple zeta valence quality for H to Rn: Design and assessment of accuracy. *Phys. Chem. Chem. Phys.* **2005,** *7*, 3297-3305.

(3) Weigend, F. Accurate Coulomb-fitting basis sets for H to Rn. *Phys. Chem. Chem. Phys.* **2006,** *8*, 1057-1065.

(4) Frisch, M. J.; Trucks, G. W.; Schlegel, H. B.; Scuseria, G. E.; Robb, M. A.; Cheeseman, J. R.; Scalmani, G.; Barone, V.; Mennucci, B.; Petersson, G. A.; Nakatsuji, H.; Caricato, M.; Li, X.; Hratchian, H. P.; Izmaylov, A. F.; Bloino, J.; Zheng, G.; Sonnenberg, J. L.; Hada, M.; Ehara, M.; Toyota, K.; Fukuda, R.; Hasegawa, J.; Ishida, M.; Nakajima, T.; Honda, Y.; Kitao, O.; Nakai, H.; Vreven, T.; Montgomery Jr., J. A.; Peralta, J. E.; Ogliaro, F.; Bearpark, M. J.; Heyd, J.; Brothers, E. N.; Kudin, K. N.; Staroverov, V. N.; Kobayashi, R.; Normand, J.; Raghavachari, K.; Rendell, A. P.; Burant, J. C.; Iyengar, S. S.; Tomasi, J.; Cossi, M.; Rega, N.; Millam, N. J.; Klene, M.; Knox, J. E.; Cross, J. B.; Bakken, V.; Adamo, C.; Jaramillo, J.; Gomperts, R.; Stratmann, R. E.; Yazyev, O.; Austin, A. J.; Cammi, R.; Pomelli, C.; Ochterski, J. W.; Martin, R. L.; Morokuma, K.; Zakrzewski, V. G.; Voth, G. A.; Salvador, P.; Dannenberg, J. J.; Dapprich, S.; Daniels, A. D.; Farkas, Ö.; Foresman, J. B.; Ortiz, J. V.; Cioslowski, J.; Fox, D. J. *Gaussian 09*, Gaussian, Inc.: Wallingford, CT, USA, 2009.